

Non-Perturbative Aspects of Spontaneous Symmetry Breaking

Jorge Gamboa¹ Justo López-Sarrión^{2,3}

¹*Departamento de Física, Universidad de Santiago de Chile, Casilla 307, Santiago, Chile*

²*Departamento de Física Teórica, Atómica y Óptica, Universidad de Valladolid, 47011 Valladolid, Spain*

³*Departamento de Física, Universidad Nacional de Colombia, 111321 Bogotá, Colombia*

E-mail: jorge.gamboa@usach.cl, jujlopezsa@unal.edu.co

ABSTRACT: Spontaneous symmetry breaking is studied in the ultralocal limit of a scalar quantum field theory, that is when $E \approx m$ (or infrared limit). In this limit we show that a φ^4 theory in the euclidean space in four-dimensions describes naturally instantons. Furthermore, in the infrared limit we show that there is an exact map between φ^4 with self-dual Yang-Mills theories. The spontaneous symmetry breaking in the infrared limit for a Higgs portal is also considered and we demonstrate how states of higher energy becomes unstable and spread converting a false vacuum in a true one.

arXiv:2009.05552v1 [hep-th] 12 Sep 2020

Contents

1	Introduction	1
2	Instantons and spontaneous symmetry breaking	3
2.1	Infrared approximation	3
2.2	Scalar and Yang-Mills theories	4
3	Higgs Portal and Vacuum	6
3.1	Global stability	7
3.2	Ground States Structure	8
3.3	Phase I	11
3.4	Phase II	11
3.5	Phases III and IV	13
3.6	Phase V	14
4	Sign changes in μ^2 parameters	15
4.1	Case $\mu_1^2 < 0$ and $\mu_2^2 > 0$	16
4.2	Case $\mu_1^2 > 0$ and $\mu_2^2 < 0$	17
4.3	Case $\mu_1^2, \mu_2^2 < 0$	18
5	Instantons and Higgs Portal	19
6	Conclusions	20

1 Introduction

In recent years an extensive discussion of how to implement the interaction between visible and dark matter [1–8] has taken place and in this discussion the role played by the Higgs portal has been fundamental [9–16]. The Higgs Portal is one of the possible prescriptions to implement the interactions between visible and dark matter in the extensions of the standard model. Among its important properties is the renormalizability and, of course, the simplicity to generate masses following the same ideas as in the conventional Higgs mechanism.

In the non-perturbative sector there are many important works since the discovery of the instanton solution [18], quantum corrections [19, 20, 22], sphaleron solution [21], θ -vacuum [23–25] and so on [26].

However, there are still other non-perturbative sectors of the standard model associated with infrared problems which are not solved and an effort in this direction is clearly necessary. From the physical point of view there are at least two reasons for us to investigate in this direction; the first, is because the interaction between visible and dark matter is very weak and non-perturbative considerations on the Higgs portal can be relevant. The second one, is because an analysis including local and global aspects of the Higgs portal is not only useful, but is also important for the analysis of spontaneous symmetry breaking and the role of vacuum beyond perturbation theory.

In this context we would like to explain the problem we will solve in this paper; the vacuum is understood in quantum field theory as the state of lowest energy from which all other many particles states are constructed. From this perspective and depending on the phenomenon, the vacuum can be unique and be the starting point for a perturbative treatment of a particular quantum field theory.

However, if there is spontaneous symmetry breaking, it could happen that perturbation theory is not applicable and the question is, how do we proceed?.

In order to explain the situation, let us start considering the Lagrangian

$$\mathcal{L} = \frac{1}{2}(\partial\varphi)^2 + V(\varphi), \quad (1.1)$$

where

$$V(\varphi) = -\frac{1}{2}\mu^2 + \frac{\lambda}{4}\varphi^4. \quad (1.2)$$

This potential has two minima

$$\varphi_0 = v = \pm\sqrt{\frac{\mu^2}{\lambda}}, \quad (1.3)$$

and an unstable extreme in $\varphi_0 = 0$.

However in the presence of spontaneous symmetry breaking the approach (perturbative) is as follows; since $v = \langle 0|\varphi|0\rangle \neq 0$, we shift φ to

$$\varphi = v + \bar{\varphi}, \quad (1.4)$$

where $\bar{\varphi}$ is a fluctuation around the vacuum v .

If the fluctuations are small, we can make perturbation theory as in the standard model, but if the minima are very deep, the low energy excitations will be “trapped” at the bottom of the wells. For the latter case the choice $+v$ or $-v$ might produce physically non-equivalent results unless a tunneling between vacua takes place [27–32].

At first glance the instantons tunneling problem would be difficult to study unless we consider field theory in $2d$ dimensions. However there is a heuristic way of looking at this problem which is by considering the infrared limit of a field theory [33].

Basically this limit implies that in the dispersion relation $E^2 = \mathbf{p}^2 + m^2$ we can assume that $E^2 \approx m^2$, and instead of the Lagrangian

$$\mathcal{L} = \frac{1}{2}(\partial\varphi)^2 - \frac{1}{2}m^2\varphi^2 + \dots,$$

we can write,

$$\mathcal{L} = \frac{1}{2}\dot{\varphi}^2 - \frac{1}{2}m^2\varphi^2 + \dots$$

in other words we neglect the spatial derivatives (more details are in the next section).

We will point out below that the infrared limit of a scalar field theory maps exactly to a Yang-Mills theory with self-dual solutions. Showing details and physical assumptions is one of the goals of this paper.

In the second part of our work, we do a global analysis for a Higgs portal and discuss the implications that this analysis has in the context explained above. So we show in the following sections how in the non-perturbative sector of the Higgs portal there is also tunneling of instantons.

The paper is organized as follows: in the next section we will explain how instantons emerge in the infrared regime, in section III and IV we will generalize our results for a Higgs Portal and analyze the structure of vacuum, in section V we will discuss the role played by the instantons in the Higgs portal description and the section VI contains the conclusions.

2 Instantons and spontaneous symmetry breaking

2.1 Infrared approximation

In order to implement the non-perturbative spontaneous symmetry mechanism, let us observe that the region that interests us is the one for which the momentum (\mathbf{p}) are very small and the ($\varphi = \varphi(t, \mathbf{x})$) field can be expanded in a Fourier series as

$$\varphi(t, \mathbf{x}) = \frac{\bar{\varphi}(t)}{\sqrt{V}} + \sum_{\mathbf{p} \neq 0} \frac{\varphi_{\mathbf{p}}}{\sqrt{V}} e^{i\mathbf{p} \cdot \mathbf{x}}. \quad (2.1)$$

where $\bar{\varphi}(t)$ only depend of t and the Lagrangean becomes

$$\begin{aligned} L &= \int d^3x \frac{1}{V} \left(\frac{1}{2} \dot{\bar{\varphi}}^2 + U(\bar{\varphi}) \right) \\ &\approx \frac{1}{2} \dot{\bar{\varphi}}^2 + U(\bar{\varphi}) + \dots, \end{aligned} \quad (2.2)$$

where \dots denotes terms that are not important for our analysis below.

Using the above arguments we see that (2.2) describes the infrared sector and to throwing away the spatial derivatives of the Lagrangian is equivalent to the ultralocal limit (infrared) [33]. This infrared limit has been used also in different contexts in quantum gravity [34–41].

Since as the spatial derivatives disappeared, the only derivatives remaining in the equations of motion are in (euclidean) time, namely

$$\ddot{\bar{\varphi}} = \mu^2 \bar{\varphi} - \lambda \bar{\varphi}^3. \quad (2.3)$$

which has the conventional instanton solution

$$\bar{\varphi}(t) = \pm \frac{\mu}{\sqrt{\lambda}} \tanh \left[\frac{\mu}{\sqrt{2}} (t - t_0) \right]. \quad (2.4)$$

Thus, the infrared limit produces the “dimensional reduction” making the excitations at very low energy instantons.

2.2 Scalar and Yang-Mills theories

In this subsection we will give direct and simple arguments to show the mapping between scalar and $SU(2)$ self-dual Yang-Mills theory.

First let us write the Lagrangian density

$$\mathcal{L} = \frac{1}{2} \dot{\varphi}^2 + \frac{\lambda}{4} \left(\varphi^2 - \frac{\mu^2}{\lambda} \right)^2,$$

in terms of dimensionless variables, defining $\varphi = \frac{\mu}{\sqrt{\lambda}} \bar{\varphi}$ where $\bar{\varphi}$ is dimensionless and we rescale $\bar{t} \rightarrow \sqrt{2} \mu t$ and the action becomes

$$S_S = \frac{1}{\lambda} \int d\bar{t} \left[\frac{1}{2} \dot{\bar{\varphi}}^2 + \frac{1}{4} (\bar{\varphi}^2 - 1)^2 \right]. \quad (2.5)$$

Now we could compare this action with the Yang-Mills one taking into account the following:

- Since the Yang-Mills description we are looking must contain instanton solutions and the self-duality condition

$$F_{\mu\nu} = \tilde{F}_{\mu\nu} \quad (2.6)$$

must be satisfied.

- If we are able to find a potential that satisfies (2.6), then we not only solve the condition (2.6) but we automatically have a solution of the Yang-Mills equations. Since in the Euclidean space $SO(4) \simeq SU(2) \times SU(2)$, the Yang-Mills potentials are a possible representation of $(\frac{1}{2}, \frac{1}{2})$ of $SU(2) \times SU(2)$.

The tensor $F_{\mu\nu}$ belong to a reducible representation $(1, 0) \oplus (0, 1)$ so that the conditions of self and anti-self dualities can be represented by the quantities

$$F_L^a = \eta_{\mu\nu}^a (F_{\mu\nu} + \tilde{F}_{\mu\nu}), \quad (2.7)$$

$$F_R^a = \bar{\eta}_{\mu\nu}^a (F_{\mu\nu} - \tilde{F}_{\mu\nu}), \quad (2.8)$$

where η and $\bar{\eta}$ are the 't Hooft symbols for $SU(2)$ which have the following properties:

$$\begin{aligned} \eta_{a\mu\nu} &= \frac{1}{2} \epsilon_{\mu\nu\rho\sigma} \eta_{a\rho\sigma}, \\ \bar{\eta}_{a\mu\nu} &= -\frac{1}{2} \epsilon_{\mu\nu\rho\sigma} \bar{\eta}_{a\rho\sigma} \\ \epsilon_{abc} \eta_{b\mu\nu} \eta_{c\rho\sigma} &= \delta_{\mu\rho} + \delta_{\nu\sigma} \eta_{\nu\sigma} \eta_{a\nu\rho} - \delta_{\nu\rho} \eta_{a\mu\sigma}, \end{aligned}$$

among other [17].

Condition (2.6) is a well-known result [18] but finding a potential that satisfies (2.6) is a highly non-trivial problem that it was solved by Diakonov in [42].

The potential is

$$A_\mu^a = \bar{\eta}_{\mu\nu}^a x_\nu \frac{[1 + \phi(x^2)]}{x^2}. \quad (2.9)$$

where ϕ a scalar field.

Replacing (2.9) in the Yang-Mills action

$$S_{YM} = -\frac{1}{4g^2} \int d^4x \text{Tr}(F_{\mu\nu}^2),$$

we find

$$S_{YM} = \frac{12\pi^2}{g^2} \int d\tau \left[\frac{1}{2} \left(\frac{d\phi}{d\tau} \right)^2 + \frac{1}{4} (\phi^2 - 1)^2 \right]. \quad (2.10)$$

The detail of this calculation is cumbersome and makes use of spherical coordinates and the fact that the measure (at $D = 4$), $dr r^{-1}$ can be written as $d\left(\ln \frac{x^2}{\rho^2}\right)$ where ρ is a scale that is introduced for dimensional reasons.

Comparing (2.5) and (2.10) we see that both actions are equivalent if

$$\lambda = \frac{g^2}{12\pi^2}, \quad (2.11)$$

with the definition $\tau = \ln \frac{x^2}{\rho^2}$.

This is a very interesting result because, on the one hand, it reveals the equivalence between scalar and self-dual Yang-Mills theories, which is an unexpected result. However, this also shows us the role played by instantons in the spontaneous symmetry breaking phenomenon at a non-perturbative level.

3 Higgs Portal and Vacuum

In this section and the next we analyze the vacuum structure of the Higgs Portal in order to apply and generalize the results in previous sections.

Let us consider two complex scalar field, we say ϕ_1 and ϕ_2 and the Lagrangian

$$\mathcal{L} = \frac{1}{2}|\partial\phi_1|^2 + \frac{1}{2}|\partial\phi_2|^2 - \frac{1}{2}\mu_1^2|\phi_1|^2 - \frac{1}{2}\mu_2^2|\phi_2|^2 + \frac{\lambda_1}{4}|\phi_1|^4 + \frac{\lambda_2}{4}|\phi_2|^4 + \frac{\gamma}{2}|\phi_1|^2|\phi_2|^2, \quad (3.1)$$

where we have introduced an interaction between the two scalar fields by the coupling γ .

For $\gamma = 0$ we have two copies of a Higgs model with symmetry breaking given by a Mexican hat potential. The classical vacuum is given for the configurations where the potential reach a minimum. However the structure of these minimal configurations will depend on the values of the parameters of the potential. Thus here we will study how structure of these minima change in the parameter space, *i.e.*, the coupling γ , the self-couplings λ_i as the couplings μ_i^2 .

The study of the regions of the parameter space which characterize certain vacuum structure is similar to the analysis of the phase diagram of a thermodynamical system with second order transitions. So, in many situations we will use the terminology of the thermodynamical phenomena in the Ginzburg-Landau theory. Thus, our analysis is similar to that of a system thermodynamical potential depending on an order parameter is characterized

by the couplings μ^2 of a quadratic term and $\lambda > 0$ of a quartic contribution. The point where the coefficient μ^2 changes of sign represents the critical point of a second order phase transition so that the ground state characterized by a vanishing (and symmetric) order parameter, changes to the situation, where the minimal configuration consists of a non-vanishing (symmetrically broken) order parameter.

We will study the possible diagram of phases in the space of the three parameters λ_i and γ fixed μ_i^2 to be positive, but we will briefly discuss how this diagram changes when other signs for μ^2 are considered.

To perform that analysis it is enough to consider only the minima of the density potential,

$$V = -\frac{1}{2}\mu_1^2|\phi_1|^2 - \frac{1}{2}\mu_2^2|\phi_2|^2 + \frac{\lambda_1}{4}|\phi_1|^4 + \frac{\lambda_2}{4}|\phi_2|^4 + \frac{\gamma}{2}|\phi_1|^2|\phi_2|^2, \quad (3.2)$$

where we have neglected the derivative terms in (3.1). In this section we will study the global stability of the model together with the phase structure depending on the parameter γ characterizing the vacuum states and their symmetries.

3.1 Global stability

To study the global stability we will search for the regions of the parameter space where the density potential (3.2) is bounded from below. Because this potential is a polynomial function on the fields, , we must look at large values of $|\phi_1|$ and $|\phi_2|$. In that region the quadratic terms are very small in comparison with the quartic terms. So we must take into account the last three terms of (3.2). A sufficient condition for the potential to be bounded is then that for any direction in the plane $|\phi_1| - |\phi_2|$ the profile of the potential is increasing with the field norm. So, if we take,

$$|\phi_2| = m|\phi_1|$$

with $m \in [0, \infty)$ being the slope which parametrizes the chosen direction, and substituting this on the quartic terms, we obtain,

$$\left(\frac{\lambda_1}{4} + \frac{\gamma}{2}m^2 + \frac{\lambda_2}{4}m^4\right)|\phi_1|^4.$$

Thus, the density potential will be globally stable if the coefficient in the expression between parenthesis is positive for the whole range of m . For the cases of $m = 0$ or $m \rightarrow \infty$ we see that λ_1 and λ_2 must be positive. Furthermore, the positivity of that coefficient will be ensured if, also, there are no real and positive zeros for m^2 . The zeros are,

$$m^2 = \frac{-\gamma \pm \sqrt{\gamma^2 - \lambda_1\lambda_2}}{\lambda_1}.$$

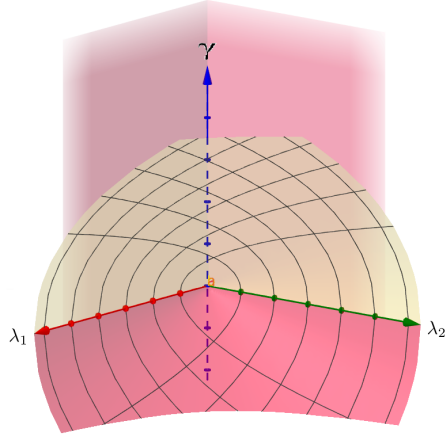


Figure 1: Region of stability in the parameter space, $\gamma > -\sqrt{\lambda_1 \lambda_2}$, $\lambda_1 > 0$ and $\lambda_2 > 0$. The boundary of the stability region are pink colored, the planes $\lambda_1 = 0$, $\lambda_2 = 0$ and the lower half-cone $\gamma = -\sqrt{\lambda_1 \lambda_2}$.

This happens when γ is positive or $\gamma^2 < \lambda_1 \lambda_2$.

Summarizing, sufficient conditions for global stability are,

$$\gamma > -\sqrt{\lambda_1 \lambda_2}, \quad \lambda_1 > 0, \quad \lambda_2 > 0. \quad (3.3)$$

Notice that the region $\gamma^2 = \lambda_1 \lambda_2$ corresponds to a cone surface in the three dimensional space $\lambda_1 - \lambda_2 - \gamma$ with the symmetrical axis being the straight line $\lambda_1 = \lambda_2$, and $\gamma = 0$ (fig. 1).

Note also that these are sufficient but no necessary conditions. The failure of these conditions can still give rise to a stable model depending on the coefficients μ_1^2 and μ_2^2 . However, in the most of our analysis we take positive values of the μ^2 factors, and the above conditions are actually necessary and sufficient.

3.2 Ground States Structure

In this section we will look for the homogeneous configurations which minimize the energy density (3.1), or equivalently, the potential density (3.2).

To do this, let us write the complex scalar fields as,

$$\phi_1 = \rho_1 e^{i\varphi_1}, \quad (3.4)$$

$$\phi_2 = \rho_2 e^{i\varphi_2}, \quad (3.5)$$

where $\rho_1, \rho_2 \geq 0$ and φ_1, φ_2 are phases. It is evident that the density potential is independent of the phases and they will not have any role in our discussion (up to the degeneracy of the possible ground states). Then, in order to find local extrema we proceed as usual by derivating with respect coordinates ρ_1 and ρ_2 , equaling them to zero and check that the hessian matrix at those points is positive definite. However, and because the domain of the variables ρ_1 and ρ_2 are not open regions we must to take into account also possible minima at the boundary ($\rho_1 = 0$, or $\rho_2 = 0$).

Hence, derivating with respect to ρ_1 and ρ_2 and equaling them to zero gives,

$$\frac{\partial V}{\partial \rho_1} = \rho_1 (-\mu_1^2 + \lambda_1 \rho_1^2 + \gamma \rho_2^2) = 0, \quad (3.6)$$

$$\frac{\partial V}{\partial \rho_2} = \rho_2 (-\mu_2^2 + \lambda_2 \rho_2^2 + \gamma \rho_1^2) = 0, \quad (3.7)$$

And the hessian matrix is,

$$\mathcal{H}(\rho_1, \rho_2) \equiv \left[\frac{\partial^2 V}{\partial \rho_i \partial \rho_j} \right] = \begin{pmatrix} -\mu_1^2 + 3\lambda_1 \rho_1^2 + \gamma \rho_2^2 & 2\gamma \rho_1 \rho_2 \\ 2\gamma \rho_1 \rho_2 & -\mu_2^2 + 3\lambda_2 \rho_2^2 + \gamma \rho_1^2 \end{pmatrix}. \quad (3.8)$$

From these last expressions it is clear the following facts:

1. With positive μ^2 's factors there will never be symmetric solutions $\rho_1 = \rho_2 = 0$ due to the negativity of the hessian (3.8).
2. we will have solutions of the form,

$$\rho_1'^2 = 2 \frac{\mu_1^2}{\lambda_1}, \quad \text{and}, \quad \rho_2'^2 = 0, \quad (3.9)$$

with positive definite hessian if,

$$\gamma > \lambda_1 \frac{\mu_2^2}{\mu_1^2}. \quad (3.10)$$

And the solution,

$$\rho_1''^2 = 0, \quad \text{and}, \quad \rho_2''^2 = 2 \frac{\mu_2^2}{\lambda_2}, \quad (3.11)$$

with positive definite hessian if,

$$\gamma > \lambda_2 \frac{\mu_1^2}{\mu_2^2}. \quad (3.12)$$

3. If ρ_1 and ρ_2 are different from zero. Then eqns (3.6) and (3.7) can be written in a matrix form,

$$\begin{pmatrix} \lambda_1 & \gamma \\ \gamma & \lambda_2 \end{pmatrix} \begin{pmatrix} \rho_1^2 \\ \rho_2^2 \end{pmatrix} = \begin{pmatrix} 2\mu_1^2 \\ 2\mu_2^2 \end{pmatrix}. \quad (3.13)$$

And hence if the 2×2 matrix is regular, then, we solve to find,

$$\rho_1^2 = \frac{\lambda_2 \mu_1^2 - \gamma \mu_2^2}{\lambda_1 \lambda_2 - \gamma^2}, \quad (3.14)$$

$$\rho_2^2 = \frac{\lambda_1 \mu_2^2 - \gamma \mu_1^2}{\lambda_1 \lambda_2 - \gamma^2}. \quad (3.15)$$

where we have to emphasize that the right hand sides must be positive to be acceptable solutions. Furthermore, on solutions of this kind the hessian matrix is reduced to,

$$\mathcal{H} = \begin{pmatrix} 2\lambda_1 \rho_1^2 & 2\gamma \rho_1 \rho_2 \\ 2\gamma \rho_1 \rho_2 & 2\lambda_2 \rho_2^2 \end{pmatrix}, \quad (3.16)$$

whose trace is always positive definite but its determinant,

$$\det \mathcal{H} = 4 (\lambda_1 \lambda_2 - \gamma^2) \rho_1^2 \rho_2^2,$$

is positive only when $\lambda_1 \lambda_2 > \gamma^2$

Hence, positivity of ρ_1^2, ρ_2^2 and the hessian \mathcal{H} occurs only if,

$$\gamma \leq \lambda_1 \frac{\mu_2^2}{\mu_1^2}, \quad \text{and}, \quad \gamma \leq \lambda_2 \frac{\mu_1^2}{\mu_2^2}. \quad (3.17)$$

4. Yet another different kind of solution happens when,

$$\gamma = \sqrt{\lambda_1 \lambda_2}, \quad \text{and}, \quad \frac{\lambda_1}{\lambda_2} = \frac{\mu_1^4}{\mu_2^4}, \quad (3.18)$$

and the values of the field modulus are not completely determined, but they lie on the elliptic curve,

$$\frac{\rho_1}{\lambda_1 \mu_1^2} + \frac{\rho_2}{\lambda_2 \mu_2^2} = \frac{2}{\lambda_1 \lambda_2}, \quad (3.19)$$

Thus, we have different possibilities which define different minima depending on the region of the parameters space. This will be analyzed in next subsections.

3.3 Phase I

If we restrict to the region,

$$\gamma > \sqrt{\lambda_1 \lambda_2}, \quad \frac{\lambda_1}{\lambda_2} = \frac{\mu_1^4}{\mu_2^4}, \quad (3.20)$$

which corresponds to a vertical half-plane over the cone $\gamma^2 = \lambda_1 \lambda_2$, as can be seen in Fig. 7, we obtain two equivalent minima at,

$$\rho_1 = \sqrt{\frac{\mu_1^2}{\lambda_1}}, \quad \rho_2 = 0,$$

and,

$$\rho_1 = 0, \quad \rho_2 = \sqrt{\frac{\mu_2^2}{\lambda_2}},$$

with potential depth,

$$V_I = -\frac{\mu_1^4}{\lambda_1} = -\frac{\mu_2^4}{\lambda_2}, \quad (3.21)$$

and with a minimal potential barrier given by,

$$\Delta V = \frac{\gamma - \sqrt{\lambda_1 \lambda_2}}{\gamma + \sqrt{\lambda_1 \lambda_2}} \frac{\mu_1^2 \mu_2^2}{\sqrt{\lambda_1 \lambda_2}}. \quad (3.22)$$

This value corresponds to a saddle point placed at,

$$\rho_1^2 = \frac{2\mu_1\mu_2}{\sqrt{\lambda_1\lambda_2} + \gamma} \left(\frac{\lambda_2}{\lambda_1} \right)^{\frac{1}{4}}, \quad (3.23)$$

$$\rho_2^2 = \frac{2\mu_1\mu_2}{\sqrt{\lambda_1\lambda_2} + \gamma} \left(\frac{\lambda_1}{\lambda_2} \right)^{\frac{1}{4}}, \quad (3.24)$$

The profile of the potential can be viewed in Fig. 2.

3.4 Phase II

The next situation corresponds to the existence of two minima, when,

$$\gamma \geq \lambda_1 \frac{\mu_2^2}{\mu_1^2}, \quad \gamma \geq \lambda_2 \frac{\mu_1^2}{\mu_2^2}, \quad (3.25)$$

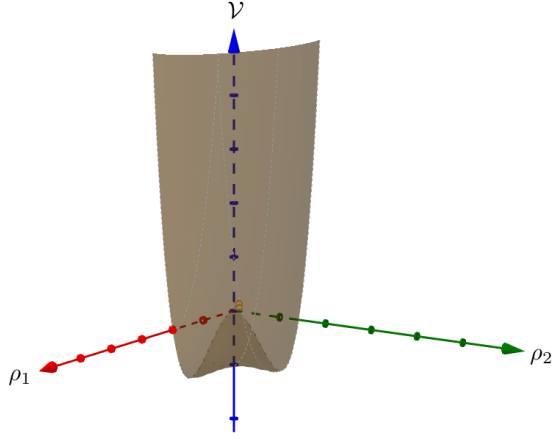


Figure 2: Profile of the potential in phase I

excluding the half-plane of the phase I. This is the region over the planes $\gamma = \lambda_1 \frac{\mu_2^2}{\mu_1}$ and $\gamma = \lambda_2 \frac{\mu_1^2}{\mu_2}$, over the cone $\gamma^2 = \lambda_1 \lambda_2$. The phase I splits the region into two pieces where there exist two vacua, a false and the true vacuum (deepest).

The left side region in Fig. 7 denoted as II, has the dominant vacuum,

$$\rho_1 = \sqrt{\frac{2\mu_1}{\lambda_1}}, \quad \rho_2 = 0, \quad (3.26)$$

with potential density,

$$V_{\text{II}} = -\frac{\mu_1^4}{\lambda}.$$

Also, this phase presents a false vacuum placed at,

$$\rho_1 = 0, \quad \rho_2 = \sqrt{\frac{2\mu_2^2}{\lambda_2}}, \quad (3.27)$$

with potential energy density,

$$V'_{\text{II}} = \frac{\mu_2^4}{\lambda_2}.$$

In the middle there is a saddle point placed at points in (3.14) and (3.15), with potential energy density,

$$V = -\frac{\lambda_1 \mu_2^4 - 2\gamma \mu_1^2 \mu_2^2 + \lambda_2 \mu_1^4}{\lambda_1 \lambda_2 - \gamma^2}. \quad (3.28)$$

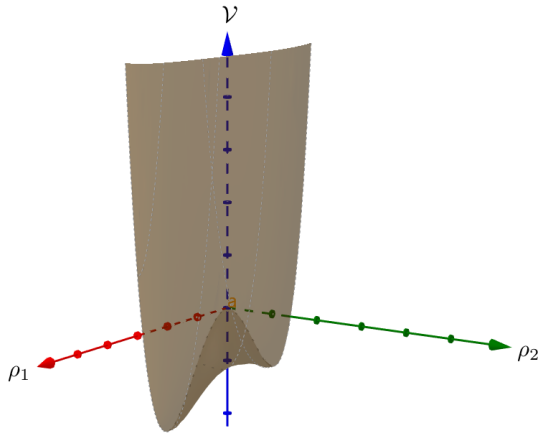


Figure 3: Profile of the potential in phase II

See Fig. 3 to check the characterization of the minima structure in this phase.

The right piece, denoted by II' in Fig. 7 is similar to the situation just above but swapping indices 1 and 2, *i.e.*, it is characterized by a dominant vacuum given by (3.27), and a false vacuum given by (3.26).

3.5 Phases III and IV

Now we analyze the situation where there occurs a unique vacuum. This happens in two situations.

The first situation, phases III and III' in Fig.7, correspond to the vacuum located at (phase III),

$$\rho_1 = 0, \quad \rho_2 = \sqrt{\frac{2\mu_2^2}{\lambda_2}},$$

when

$$\lambda_2 \frac{\mu_1^2}{\mu_1^2} < \gamma < \lambda_1 \frac{\mu_2^2}{\mu_1^2}$$

or (phase III'),

$$\rho_1 = \sqrt{\frac{2\mu_2^1}{\lambda_1}}, \quad \rho_2 = 0,$$

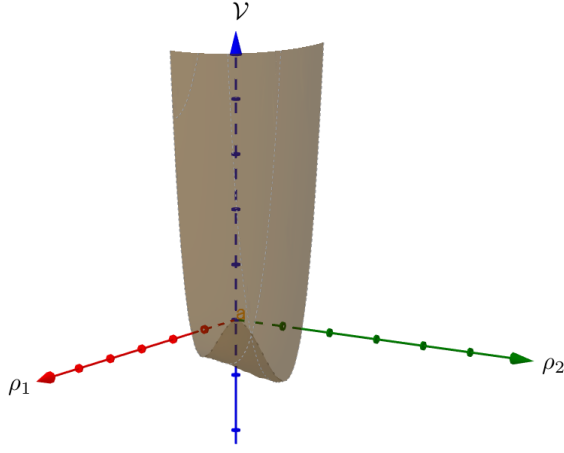


Figure 4: Profile of the potential in phase III

when,

$$\lambda_1 \frac{\mu_2^2}{\mu_1^2} < \gamma < \lambda_2 \frac{\mu_1^2}{\mu_2^2}$$

respectively, with minimal potential energies given in previous subsection. See Fig.4 for the potential profile of this phase.

The second situation, phase IV in Fig. 7 happens when,

$$\gamma \leq \lambda_1 \frac{\mu_2^2}{\mu_1^2}, \quad \gamma \leq \lambda_2 \frac{\mu_1^2}{\mu_2^2},$$

with the unique minimum placed at position given in (3.14) and (3.15) and with potential depth given in (3.28), see Fig. 5.

3.6 Phase V

Finally we obtain an degenerate vacuum when,

$$\gamma = \sqrt{\lambda_1 \lambda_2}, \quad \frac{\lambda_1}{\lambda_2} = \frac{\mu_1^4}{\mu_2^4},$$

which is a straight line corresponding to a generatrix of the cone $\gamma^2 = \lambda_1 \lambda_2$. The vacuum is degenerate along the elliptic curve (3.19) and its depth potential is,

$$V = -\frac{\mu_1^2 \mu_2^2}{\sqrt{\lambda_1 \lambda_2}},$$

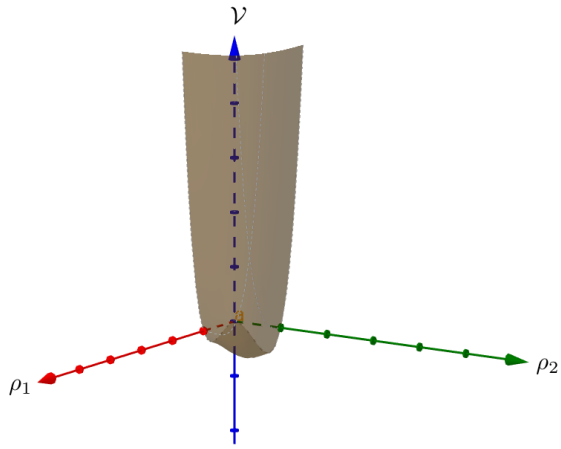


Figure 5: Profile of the potential in phase I V

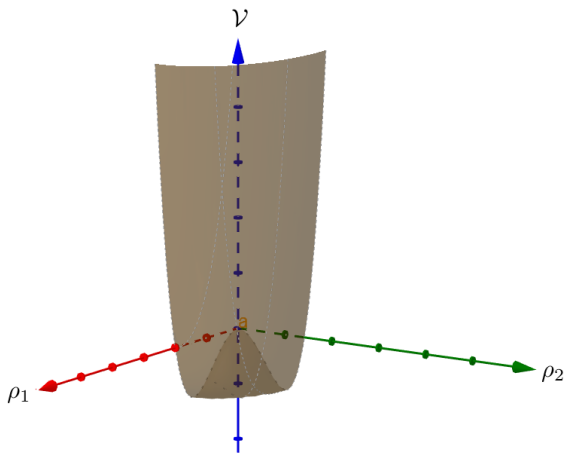


Figure 6: Profile of the potential in phase V

see Fig. 6.

4 Sign changes in μ^2 parameters

In this section we complete the previous analysis for the cases where parameters μ_1^2 and/or μ_2^2 change sign.

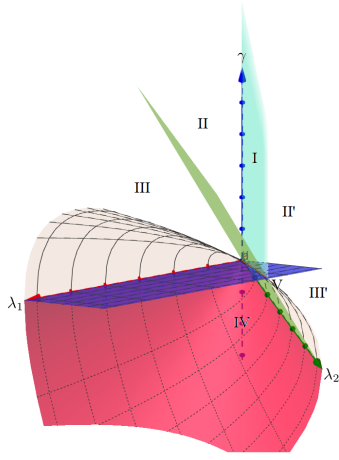


Figure 7: Diagram of phases in 3D ($\lambda_1 - \lambda_2 - \gamma$).

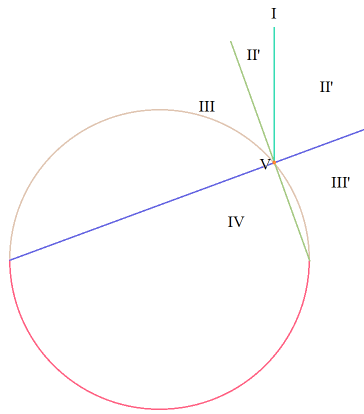


Figure 8: Transversal section of the phase diagram with respect to a plane perpendicular to the symmetric axis of the cone ($\lambda_1 = \lambda_2$).

4.1 Case $\mu_1^2 < 0$ and $\mu_2^2 > 0$

Firstly, in this case the symmetric solution $\rho_1 = \rho_2 = 0$ is a saddle point as it can be seen directly from (3.8).

The solutions of the kind $\rho_1 = 0$ and $\rho_2 \neq 0$, namely,

$$\rho_2^2 = \frac{2\mu_2^2}{\lambda_2},$$

can be realized as minima if,

$$\gamma > \lambda_2 \frac{\mu_1^2}{\mu_2^2}, \quad (4.1)$$

as it can be seen from the expression of the hessian (3.8). Obviously solutions of the form $\rho_2 = 0$ and $\rho_1 \neq 0$ can not be realized.

Now let us analyze the case $\rho_1 \neq 0$ and $\rho_2 \neq 0$. In order to have non vanishing solutions we impose that expressions (3.14) and (3.15) to be positive, so that we arrive to the inequalities inside the cone,

$$\gamma < \lambda_2 \frac{\mu_1^2}{\mu_2^2}, \quad \gamma > \lambda_1 \frac{\mu_2^2}{\mu_1^2}, \quad -\sqrt{\lambda_1 \lambda_2} < \gamma < \sqrt{\lambda_1 \lambda_2}, \quad (4.2)$$

and this is a non empty region of parameters, and furthermore, for the solutions belonging to this set of inequalities we have a positive definite Hessian as it can be seen from (3.16). So in this region, the vacuum expectation values are given by (3.14) and (3.15), Also we must look outside the cone $\gamma > \sqrt{\lambda_1 \lambda_2}$, and we find the inequalities,

$$\gamma > \lambda_2 \frac{\mu_1^2}{\mu_2^2}, \quad \gamma < \lambda_1 \frac{\mu_2^2}{\mu_1^2}, \quad \gamma > \sqrt{\lambda_1 \lambda_2}, \quad (4.3)$$

Clearly this set of inequalities are incompatible, and there is no solution of this kind outside the cone.

Hence the phase space is simple in this case: we have a phase of type IV inside the cone and below the plane $\gamma = \lambda_2 \frac{\mu_1^2}{\mu_2^2}$, see Fig. 9, and phase of type III' on the rest of space parameters with stability.

4.2 Case $\mu_1^2 > 0$ and $\mu_2^2 < 0$

This case is entirely similar to the case above but swapping indices 1 and 2. the phase space is drawn in Fig. 10. Note that the phase IV has changed its location and phase III appears instead of phase III'.

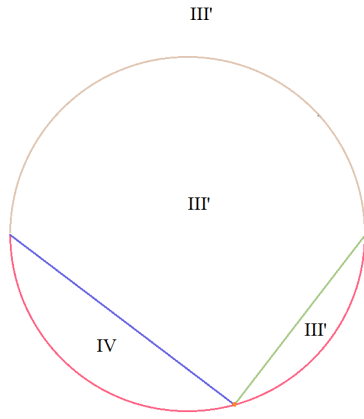


Figure 9: Phase diagram for $\mu_1^2 < 0$.

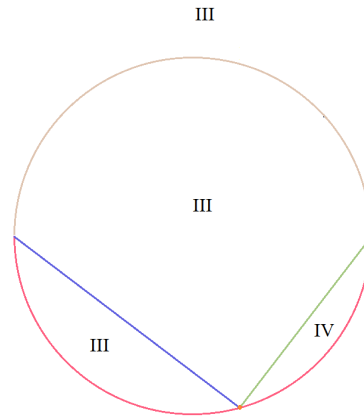


Figure 10: Phase diagram for $\mu_2^2 < 0$.

4.3 Case $\mu_1^2, \mu_2^2 < 0$

It is easy to see that in this case, if we assume that $\gamma^2 < \lambda_1 \lambda_2$, the region for ρ_1^2 and ρ_2^2 being positive in (3.14) and (3.15) is that above both planes $\gamma = \lambda_2 \frac{\mu_1^2}{\mu_2^2}$ and $\gamma = \lambda_1 \frac{\mu_2^2}{\mu_1^2}$, and hence there is no way to have the phase *I* outside the cone. Furthermore, by setting any of the ρ 's to zero, the other can not reach a minimum. Hence the only possibility for the

minimum is,

$$\rho_1 = 0, \quad \rho_2 = 0, \quad (4.4)$$

which corresponds to the maximal symmetric vacuum. Similar situation occurs outside the cone, and only symmetric solution is possible.

5 Instantons and Higgs Portal

In this section we generalize the results given in III and IV for the Higgs portal (3.1). More specifically in phase I we have two minima separated by a potential barrier while in phases II and II' there are two asymmetric minima, one of them is a false vacuum.

These two cases are of interest by the following reasons:

- Potential I is the classical Mexican hat potential for which spontaneous symmetry breaking is restored by instantons effects.
- The potential II and II' is metastable and decays to a true vacuum. However, when it decays to true vacuum, it transfers information about the physical parameters to true vacuum.

Interestingly the two cases mentioned above can be analyzed in the infrared limit assuming the boundary condition

$$\lim_{|x| \rightarrow \infty} \varphi_{1,2}(x) \rightarrow \pm v_{1,2}. \quad (5.1)$$

The equation of motion are

$$\ddot{\varphi}_1 = -\mu_1^2 \varphi_1 + \lambda_1 |\varphi_1|^2 \varphi_1 + \gamma |\varphi_2|^2 \varphi_1, \quad (5.2)$$

$$\ddot{\varphi}_2 = -\mu_2^2 \varphi_2 + \lambda_2 |\varphi_2|^2 \varphi_2 + \gamma |\varphi_1|^2 \varphi_2. \quad (5.3)$$

Although we cannot solve these equations analytically, we can try to find asymptotic solutions using the fact that both φ_1 and φ_2 tend to v_1 and v_2 . Using the condition (5.1) and the fact that

$$v_1^2 = \frac{-\lambda_2 \mu_1^2 + \gamma \mu_2^2}{\gamma^2 - \lambda_1 \lambda_2}, \quad (5.4)$$

$$v_2^2 = \frac{-\lambda_1 \mu_2^2 + \gamma \mu_1^2}{\gamma^2 - \lambda_1 \lambda_2}, \quad (5.5)$$

The first and second equations become

$$\begin{aligned}\ddot{\varphi}_1 &= -(\mu_1^2 - \gamma v_2^2) \varphi_1 + \lambda_1 |\varphi_1|^2 \varphi_1, \\ \ddot{\varphi}_2 &= -(\mu_2^2 - \gamma v_1^2) \varphi_2 + \lambda_2 |\varphi_2|^2 \varphi_2.\end{aligned}\tag{5.6}$$

or in terms of the effective parameters

$$\begin{aligned}\tilde{\mu}_1^2 &= (\mu_1^2 - \gamma v_2^2) = \frac{\lambda_1(\gamma\mu_2^2 - \lambda_2\mu_1^2)}{\gamma^2 - \lambda_1\lambda_2} \\ \tilde{\mu}_2^2 &= (\mu_2^2 - \gamma v_1^2) = \frac{\lambda_2(\gamma\mu_1^2 - \lambda_1\mu_2^2)}{\gamma^2 - \lambda_1\lambda_2}.\end{aligned}\tag{5.7}$$

Then the asymptotic solutions are

$$\bar{\varphi}_1(t) = \pm \sqrt{\frac{\tilde{\mu}_1^2}{\lambda_1}} \tanh \left[\sqrt{\frac{\tilde{\mu}_1^2}{2}} (t - t_0) \right],\tag{5.8}$$

$$\bar{\varphi}_2(t) = \pm \sqrt{\frac{\tilde{\mu}_2^2}{\lambda_2}} \tanh \left[\sqrt{\frac{\tilde{\mu}_2^2}{2}} (t - t_0) \right],\tag{5.9}$$

which are two uncoupled (dilute) instantons with effective parameters $(\tilde{\mu}_1, \lambda_1)$ and $(\tilde{\mu}_2, \lambda_2)$ respectively.

The stability of the vacua in the Higgs portal must satisfy

$$\tilde{\mu}_1^2 > 0, \quad \tilde{\mu}_2^2 > 0.\tag{5.10}$$

If $\tilde{\mu}_1^2 = \tilde{\mu}_2^2 > 0$, then the spontaneous symmetry breaking is restored by tunneling of instantons and if $\tilde{\mu}_1^2 \neq \tilde{\mu}_2^2 > 0$, the state of higher energy becomes unstable through barrier penetration and this is an example of a false vacuum [28].

These conclusions are reached from the analysis of sections III and IV.

6 Conclusions

We summarize the main results obtained:

a) We have studied the spontaneous symmetry breaking phenomenon at the infrared limit, motivated especially by the need to understand low energy physics and tunneling phenomena between vacuums. The φ^4 -theory has been considered and we have shown that instantons play a relevant role. The appearance of instantons in the infrared limit is natural because by eliminating the spatial derivatives the system becomes an infinite degrees of

freedom quantum mechanics problem.

b) For Higgs Portal type potentials the analysis is somewhat more complicated although much richer, the vacua has properties that mix physical content from the different coupling constants and effective masses.

A field theory at the infrared limit has, in our opinion, a good chance of being physically interesting due to the physical content that could be extracted from it. The appearance of instantons, false vacua and tunneling are not *a priori* obvious results.

Although we have not explored in detail beyond what we have discussed in this paper, it seems to us that the idea of looking at very low energy sectors in the context discussed in this paper can yield insights into dark matter physics.

Acknowledgements

We would like to acknowledge the discussions and suggestions of J. L. Cortés, H. Falomir, F. A. Schaposnik and F. Méndez. This work was partially supported by Dicyt 041831GR (J.G.), and by Fundacion ONCE with grant *Oportunidad al Talento* (J.L.S.).

References

- [1] G. Bertone and D. Hooper, *Rev. Mod. Phys.* **90** (2018) no.4, 045002.
- [2] D. Carney, G. Krnjaic, D. C. Moore, C. A. Regal, G. Afek, S. Bhave, B. Brubaker, T. Corbitt, J. Cripe, N. Crisosto, A. Geraci, S. Ghosh, J. G. E. Harris, A. Hook, E. W. Kolb, J. Kunjummen, R. F. Lang, T. Li, T. Lin, Z. Liu, J. Lykken, L. Magrini, J. Manley, N. Matsumoto, A. Monte, F. Monteiro, T. Purdy, C. J. Riedel, R. Singh, S. Singh, K. Sinha, J. M. Taylor, J. Qin, D. J. Wilson and Y. Zhao, [arXiv:2008.06074 [physics.ins-det]].
- [3] I. de Martino, S. S. Chakrabarty, V. Cesare, A. Gallo, L. Ostorero and A. Diaferio, *Universe* **6** (2020) no.8, 107 doi:10.3390/universe6080107 [arXiv:2007.15539 [astro-ph.CO]].
- [4] E. Ferreira, G.M., [arXiv:2005.03254 [astro-ph.CO]].
- [5] C. Miller, A. L. Erickcek and R. Murgia, *Phys. Rev. D* **100** (2019) no.12, 123520
- [6] G. Bertone, D. Hooper and J. Silk, *Phys. Rept.* **405** (2005), 279-390
- [7] R. Engel *et al.* [FUNK Experiment], [arXiv:1711.02961 [hep-ex]].
- [8] P. A. Zyla *et al.* [Particle Data Group], *PTEP* **2020** (2020) no.8, 083C01
- [9] B. Patt and F. Wilczek, [arXiv:hep-ph/0605188 [hep-ph]].
- [10] G. Ballesteros, J. Redondo, A. Ringwald and C. Tamarit, *JCAP* **08** (2017), 001

- [11] A. Falkowski, C. Gross and O. Lebedev, *JHEP* **05** (2015), 057.
- [12] A. Eichhorn and M. Pauly, [arXiv:2005.03661 [hep-ph]].
- [13] M. Chianese, B. Fu and S. F. King, *JCAP* **06** (2020), 019. .
- [14] C. Englert, J. Jaeckel, M. Spannowsky and P. Stylianou, *Phys. Lett. B* **806** (2020), 135526
- [15] G. Arcadi, A. Djouadi and M. Raidal, *Phys. Rept.* **842** (2020), 1-180.
- [16] A. Filimonova and S. Westhoff, *JHEP* **02** (2019), 140
- [17] A. V. Belitsky, S. Vandoren and P. van Nieuwenhuizen, *Class. Quant. Grav.* **17** (2000), 3521-3570
- [18] A. A. Belavin, A. M. Polyakov, A. S. Schwartz and Y. S. Tyupkin, *Phys. Lett. B* **59** (1975), 85-87.
- [19] G. 't Hooft, *Phys. Rev. D* **14**, 3432 (1976) Erratum: [*Phys. Rev. D* **18**, 2199 (1978)].
- [20] G. 't Hooft, *Phys. Rept.* **142** (1986), 357-387
- [21] F. R. Klinkhamer and N. S. Manton, *Phys. Rev. D* **30** (1984), 2212.
- [22] F. A. Schaposnik, *Phys. Rev. D* **18** (1978), 1183-1191.
- [23] C. G. Callan, Jr., R. F. Dashen and D. J. Gross, *Phys. Lett. B* **63** (1976), 334-340
- [24] R. Jackiw and C. Rebbi, *Phys. Rev. Lett.* **37** (1976), 172-175.
- [25] R. Jackiw and C. Rebbi, *Phys. Rev. D* **13** (1976), 3398-3409.
- [26] For a review on classical Yang-Mills solutions see for example, A. Actor, *Rev. Mod. Phys.* **51** (1979), 461
- [27] A. M. Polyakov, *Nucl. Phys. B* **120** (1977), 429-458.
- [28] S. R. Coleman, *Phys. Rev. D* **15** (1977), 2929-2936.
- [29] C. G. Callan, Jr. and S. R. Coleman, *Phys. Rev. D* **16** (1977), 1762-1768.
- [30] S. R. Coleman, *Subnucl. Ser.* **15**, 805 (1979).
- [31] M. B. Paranjape, "The Theory and Applications of Instanton Calculations", Cambridge University Press (2017).
- [32] E. Fradkin, *Lectures Notes on Quantum Field Theory*, Chap 9, UIUC (unpublished).
- [33] J. R. Klauder, *Commun. Math. Phys.* **18** (1970), 307-318
- [34] M. Pilati, *Phys. Rev. D* **28**, 729 (1983).
- [35] M. Henneaux, M. Pilati and C. Teitelboim, *Phys. Lett.* **110B**, 123 (1982).
- [36] C. Teitelboim, *Phys. Rev. D* **25**, 3159 (1982).
- [37] J. Gamboa, *Phys. Rev. Lett.* **74**, 1900 (1995).
- [38] J. Gamboa and F. Mendez, *Nucl. Phys. B* **600**, 378 (2001).

- [39] J. Gamboa, Phys. Rev. D **53**, 6991 (1996)
- [40] C. J. Isham, IMPERIAL/TP/88-89/30.
- [41] E. Anderson, Gen. Rel. Grav. **36** (2004), 255-276
- [42] D. Diakonov, Prog. Part. Nucl. Phys. **51** (2003), 173-222